

# Electron capture rates on nuclei and implications for stellar core collapse

K. Langanke,<sup>1</sup> G. Martínez-Pinedo,<sup>2,3</sup> J. M. Sampaio,<sup>1</sup> D. J. Dean,<sup>4</sup> W. R. Hix,<sup>4,5,6</sup>  
O. E. B. Messer,<sup>4,5,6</sup> A. Mezzacappa,<sup>4</sup> M. Liebendörfer,<sup>7,4,5</sup> H.-Th. Janka,<sup>8</sup> and M. Rampp<sup>8</sup>

<sup>1</sup>*Institute for Physics and Astronomy, University of Århus, DK-8000 Århus C, Denmark*

<sup>2</sup>*Institut d'Estudis Espacials de Catalunya, Edifici Nexus, Gran Capità 2, E-08034 Barcelona, Spain*

<sup>3</sup>*Institució Catalana de Recerca i Estudis Avançats, Lluís Companys 23, E-08010 Barcelona, Spain*

<sup>4</sup>*Physics Division, Oak Ridge National Laboratory, Oak Ridge, TN 37831*

<sup>5</sup>*Department of Physics and Astronomy, University of Tennessee, Knoxville TN 37996*

<sup>6</sup>*Joint Institute for Heavy Ion research, Oak Ridge, TN 37831*

<sup>7</sup>*Canadian Institute for Theoretical Astrophysics, Toronto ON M5S 3H8*

<sup>8</sup>*Max-Planck-Institut für Astrophysik, D-85741 Garching, Germany*

(Dated: October 31, 2018)

Supernova simulations to date have assumed that during core collapse electron captures occur dominantly on free protons, while captures on heavy nuclei are Pauli-blocked and are ignored. We have calculated rates for electron capture on nuclei with mass numbers  $A = 65$ –112 for the temperatures and densities appropriate for core collapse. We find that these rates are large enough so that, in contrast to previous assumptions, electron capture on nuclei dominates over capture on free protons. This leads to significant changes in core collapse simulations.

PACS numbers: 26.50.+x, 97.60.Bw, 23.40.-s

At the end of their lives, stars with masses exceeding roughly  $10 M_{\odot}$  reach a moment in their evolution when their iron core provides no further source of nuclear energy generation. At this time, they collapse and, if not too massive, bounce and explode in spectacular events known as type II or Ib/c supernovae. As the density,  $\rho$ , of the star's center increases, electrons become more degenerate and their chemical potential  $\mu_e$  grows ( $\mu_e \sim \rho^{1/3}$ ). For sufficiently high values of the chemical potential electrons are captured by nuclei producing neutrinos, which for densities  $\lesssim 10^{11} \text{ g cm}^{-3}$ , freely escape from the star, removing energy and entropy from the core. Thus the entropy stays low during collapse ensuring that nuclei dominate in the composition over free protons and neutrons. During the presupernova stage, i.e. for core densities  $\lesssim 10^{10} \text{ g cm}^{-3}$  and proton-to-nucleon ratios  $Y_e \gtrsim 0.42$ , nuclei with  $A = 55$ –65 dominate. The relevant rates for weak-interaction processes (including  $\beta^{\pm}$  decay and electron and positron capture) were first estimated by Fuller, Fowler and Newman [1] (for nuclei with  $A < 60$ ), considering that at such conditions allowed (Fermi and Gamow-Teller) transitions dominate. The rates have been recently improved based on modern data and state-of-the-art many-body models [2], considering nuclei with  $A = 45$ –65. (This rate set will be denoted LMP in the following.) Presupernova models utilizing these improved weak rates are presented in [3]. In collapse simulations, i.e. densities  $\gtrsim 10^{10} \text{ g cm}^{-3}$ , a much simpler description of electron capture on nuclei is used. Here the rates are estimated in the spirit of the independent particle model (IPM), assuming pure Gamow-Teller (GT) transitions and considering only single particle states for proton and neutron numbers between  $Z, N = 20$ –40 [4]. In particular this model results

in vanishing electron capture rates on nuclei with neutron numbers larger than  $N = 40$ , motivated by the observation [5] that, within the IPM, GT transitions are Pauli-blocked for nuclei with  $N \geq 40$  and  $Z \leq 40$ .

During core collapse, temperatures and densities are high enough to ensure that nuclear statistical equilibrium (NSE) is achieved. This means that for sufficiently low entropies, the matter composition is dominated by the nuclei with the highest binding energy for a given  $Y_e$ . Electron capture reduces  $Y_e$ , driving the nuclear composition to more neutron rich and heavier nuclei, including those with  $N > 40$ , which dominate the matter composition for densities larger than a few  $10^{10} \text{ g cm}^{-3}$ . As a consequence of the model applied in previous collapse simulations, electron capture on nuclei ceases at these densities and the capture is entirely due to free protons. We will show now that the employed model for electron capture on nuclei is incorrect, as the Pauli-blocking of the GT transitions is overcome by correlations [6] and temperature effects [5, 7].

The residual nuclear interaction, beyond the IPM, mixes the  $pf$  shell with the levels of the  $sdg$  shell, in particular with the lowest orbital,  $g_{9/2}$ . This makes the closed  $g_{9/2}$  orbit a magic number in stable nuclei ( $N = 50$ ) and introduces, for example, a very strong deformation in the  $N = Z = 40$  nucleus  $^{80}\text{Zr}$ . Moreover, the description of the  $B(E2, 0^+ \rightarrow 2_1^+)$  transition in  $^{68}\text{Ni}$  requires configurations where more than one neutron is promoted from the  $pf$  shell into the  $g_{9/2}$  orbit [8], unblocking the GT transition even in this proton-magic  $N = 40$  nucleus. Such a non-vanishing GT strength has already been observed for  $^{72}\text{Ge}$  ( $N = 40$ ) [9] and  $^{76}\text{Se}$  ( $N = 42$ ) [10]. In addition, during core collapse electron capture on the nuclei of interest occurs at temperatures

$T \gtrsim 0.8$  MeV, which, in the Fermi gas model, corresponds to a nuclear excitation energy  $U \approx AT^2/8 \gtrsim 5$  MeV; this energy is noticeably larger than the splitting of the  $pf$  and  $sdg$  orbitals ( $E_{g_{9/2}} - E_{p_{1/2}, f_{5/2}} \approx 3$  MeV). Hence, the configuration mixing of  $sdg$  and  $pf$  orbitals will be rather strong in those excited nuclear states of relevance for stellar electron capture. Furthermore, the nuclear state density at  $E \sim 5$  MeV is already larger than 100/MeV, making a state-by-state calculation of the rates impossible, but also emphasizing the need for a nuclear model which describes the correlation energy scale at the relevant temperatures appropriately. This model is the Shell Model Monte Carlo (SMMC) approach [11] which allows the calculations of nuclear properties at finite temperature in unprecedentedly large model spaces. To calculate electron capture rates for nuclei  $A = 65-112$  we have first performed SMMC calculations in the full  $pf$ - $sdg$  shell, using a residual pairing+quadrupole interaction, which, in this model space, reproduces well the collectivity around the  $N = Z = 40$  region and the observed low-lying spectra in nuclei like  $^{64}\text{Ni}$  and  $^{64}\text{Ge}$ . From the SMMC calculations we determined the temperature-dependent occupation numbers of the various single-particle orbitals, which then became the input in RPA calculations of the capture rate, where we considered allowed and forbidden transitions up to multipoles  $J = 4$ , including the momentum dependence of the operators. This model is described in more details in [6], where, however, a smaller model space has been used.

To validate our method at the early collapse conditions, we have performed diagonalization shell model studies for  $^{64,66}\text{Ni}$ , considering the complete ( $pf$ ) shell for  $^{64}\text{Ni}$ , and adopting, for  $^{66}\text{Ni}$ , the ( $pf$ ) shell for protons and the ( $pf_{5/2}g_{9/2}$ ) shell for neutrons. We find agreement to better than a factor 2 between the present (SMMC+RPA) rates and the diagonalization shell model rates at stellar conditions ( $T \lesssim 0.8$  MeV), for which the latter can still be evaluated.

For all studied nuclei we find neutron holes in the ( $pf$ ) shell and, for  $Z > 30$ , non-negligible proton occupation numbers for the  $sdg$  orbitals. This unblocks the GT transitions and leads to sizable electron capture rates. Fig. 1 compares the electron capture rates for free protons and selected nuclei along a core collapse trajectory, as taken from [12]. Depending on their proton-to-nucleon ratio  $Y_e$  and their  $Q$ -values, these nuclei are abundant at different stages of the collapse. For all nuclei, the rates are dominated by GT transitions at low densities, while forbidden transitions contribute sizably for  $\gtrsim 10^{11}$  g cm $^{-3}$ . The electron chemical potential  $\mu_e$  and the reaction  $Q$ -value are the two important energy scales of the capture process. At a given density, i.e. constant  $\mu_e$ , the rate is generally larger for nuclei with smaller  $Q$ -values. The rate is sensitive to the GT strength distribution, if  $\mu_e \lesssim Q$ . However,  $\mu_e$  increases much faster with density than the  $Q$ -values of the abundant nuclei. As a consequence the

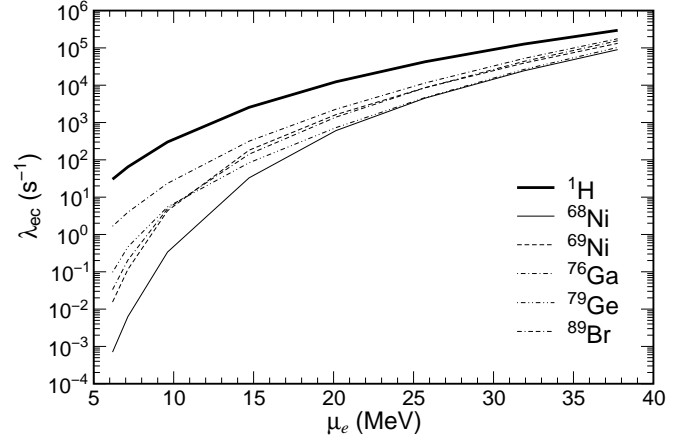


FIG. 1: Comparison of the electron capture rates on free protons and selected nuclei as function of the electron chemical potential along a stellar collapse trajectory taken from [12]. Neutrino blocking of the phase space is not included in the calculation of the rates.

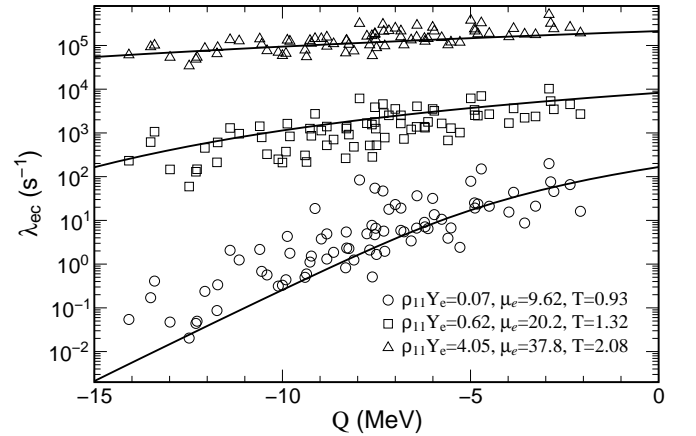


FIG. 2: Electron capture rates on nuclei as function of  $Q$ -value for 3 different stellar conditions. Temperature and electron chemical potential are measured in MeV. The solid lines represent the approximate  $Q$ -dependence of the rates as defined in Eq. (1). Neutrino blocking of the phase space is not included in the calculation of the rates.  $\rho_{11}$  measures the density in units of  $10^{11}$  g cm $^{-3}$ .

capture rates on nuclei become quite similar at larger densities, say  $\gtrsim 10^{11}$  g cm $^{-3}$ , depending now basically only on the total GT strength, but not its detailed distribution. This is demonstrated in Fig. 2 which shows our calculated capture rates as function of  $Q$ -value at 3 different stellar conditions. The  $Q$ -value dependence of the capture rate for a transition from a parent state at excitation energy  $E_i$  to a daughter state at  $E_f$  ( $\Delta E = E_f - E_i$ )

is well approximated by [13]

$$\lambda = \frac{(\ln 2)B}{K} \left( \frac{T}{m_e c^2} \right)^5 [F_4(\eta) - 2\chi F_3(\eta) + \chi^2 F_2(\eta)] \quad (1)$$

where  $\chi = (Q - \Delta E)/T$ ,  $\eta = (\mu_e + Q - \Delta E)/T$ ,  $K = 6146$  s and  $B$  represents a typical (Gamow-Teller plus forbidden) matrix element. The quantities  $F_k$  are the relativistic Fermi integrals of order  $k$ .

At ( $\rho Y_e = 7 \times 10^9$  g cm $^{-3}$ ,  $T = 0.93$  MeV), we observe some scatter of the calculated rates around the mean  $Q$ -dependence indicating that several parent and daughter states with different transition strengths contribute. For nuclei with large  $|Q|$ -values the simple parametrization breaks down. However, at  $\rho_{11} Y_e \gtrsim 4$ , the electron chemical potential has increased sufficiently that the rates become virtually independent of the strength distribution and are well represented by the average  $Q$ -value dependence (1) with  $B = 4.6$  and  $\Delta E = 2.5$  MeV. Such a parametrization could then be adopted in core collapse simulations for even higher densities, when nuclei heavier than the ones included in the present study start to dominate in the composition.

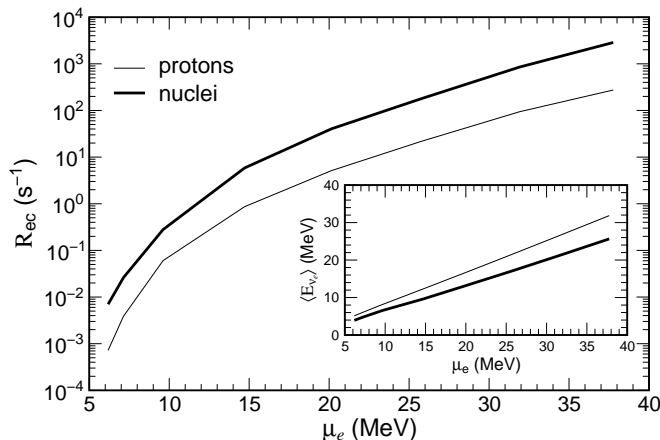


FIG. 3: The reaction rates for electron capture on protons (thin line) and nuclei (thick line) are compared as a function of electron chemical potential along a stellar collapse trajectory taken from [12]. The insert shows the related average energy of the neutrinos emitted by capture on nuclei and protons. The results for nuclei are averaged over the full nuclear composition (see text). Neutrino blocking of the phase space is not included in the calculation of the rates.

Simulations of core collapse require reaction rates for electron capture on protons,  $R_p = Y_p \lambda_p$ , and nuclei  $R_h = \sum_i Y_i \lambda_i$  (where the sum runs over all the nuclei present and  $Y_i$  denotes the number abundance of a given species), over wide ranges in density and temperature. While  $R_p$  is readily derived from [4], the calculation of  $R_h$  requires knowledge of the nuclear composition, in addition to the electron capture rates described earlier. The information about the nuclear composition

provided by the commonly used Lattimer-Swesty equation of state [14], the total abundance of heavy nuclei and the average  $Z$  and  $A$ , is not sufficiently detailed to make adequate use of these new reaction rates. Therefore a Saha-like NSE is used to calculate the needed abundances of individual isotopes, including Coulomb corrections to the nuclear binding energy [15, 16], but neglecting the effects of degenerate nucleons [17]. The combination of this NSE with electron capture rates for approximately 200 nuclei with  $A = 45$ –112, which we have determined here and in Ref. [2], was used to compute the rate of electron capture on nuclei and the emitted neutrino spectra as a function of temperature, density and electron fraction. This is similar to treatments used in investigations of electron capture during stellar evolution [3] and in thermonuclear supernovae [18]. The rates for the inverse neutrino-absorption process are determined from the electron capture rates by detailed balance. Due to its much smaller  $|Q|$ -value, the electron capture rate on the free protons is larger than the rates of abundant nuclei during the core collapse (fig. 1). However, this is misleading as the low entropy keeps the protons significantly less abundant than heavy nuclei during the collapse. Fig. 3 shows that the reaction rate on nuclei,  $R_h$ , dominates the one on protons,  $R_p$ , by roughly an order of magnitude throughout the collapse when the composition is considered. Only after the bounce shock has formed does  $R_p$  become higher than  $R_h$ , due to the high entropies and high temperatures in the shock-heated matter that result in a high proton abundance. The obvious conclusion is that electron capture on nuclei must be included in collapse simulations.

It is also important to stress that electron capture on nuclei and on free protons differ quite noticeably in the neutrino spectra they generate. The average neutrino energy,  $\langle E_\nu \rangle$ , of the neutrinos emitted by electron capture on nuclei, can be obtained dividing the neutrino energy loss rate (defined by  $\sum_i Y_i \mathcal{E}_i$  where  $\mathcal{E}_i$  is the energy loss rate by electron capture on nucleus  $i$  and  $Y_i$  denotes its number abundance) by the reaction rate for electron capture on nuclei,  $R_h$ . For the neutrino spectrum we adopt the parametrized form as defined in [19], adjusted to reproduce the average neutrino energy  $\langle E_\nu \rangle$ . The neutrino emissivity is then obtained by multiplying the NSE-averaged electron capture rate by the neutrino spectra.

Fig. 3 demonstrates that neutrinos from captures on nuclei have a mean energy 40–60% less than those produced by capture on protons. Although capture on nuclei under stellar conditions involves excited states in the parent and daughter nuclei, it is mainly the larger  $|Q|$ -value which significantly shifts the energies of the emitted neutrinos to smaller values. Despite that, the total neutrino energy loss rate is larger when electron capture on nuclei is considered, caused by the increase in the total (nuclei plus protons) electron capture rate. The differences in

the neutrino spectra strongly influence neutrino-matter interactions, which scale with the square of the neutrino energy and are essential for collapse simulations. In current simulations [12, 20], the low energy portions of the neutrino distribution are populated via neutrino-electron inelastic scattering of high energy neutrinos produced by electron capture on free protons. Electron capture on nuclei produces neutrinos with significantly lower energies, accelerating this redistribution process. In this context, inelastic neutrino-nucleus scattering, which is usually ignored, could also be an important process [21, 22].

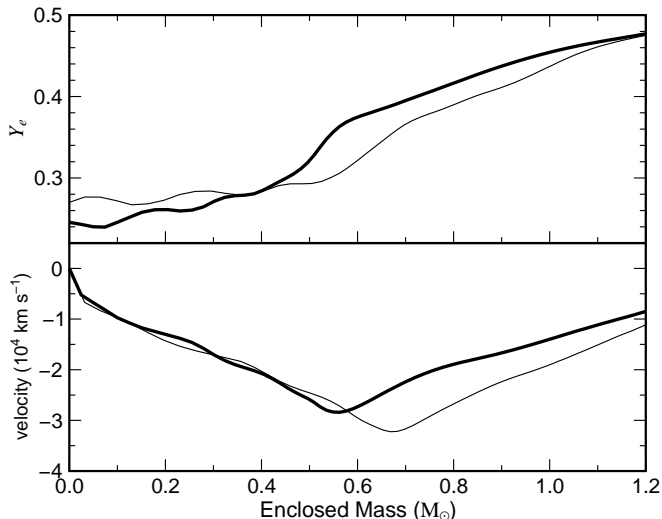


FIG. 4: The electron fraction and velocity as functions of the enclosed mass at the moment when the center reaches nuclear matter densities for a  $15 M_{\odot}$  model [3]. The thin line is a simulation using the Bruenn parameterization [4] while the thick line is for a simulation using the combined LMP [2] and SMMC+RPA rate sets. Both models were calculated with Newtonian gravity.

The effects of this more realistic implementation of electron capture on heavy nuclei have been evaluated in independent self-consistent neutrino radiation hydrodynamics simulations by the Oak Ridge and Garching collaborations [23, 24]. The basis of these models is described in detail in Refs. [12] and [20]. Both collapse simulations yield qualitatively the same results. Here we show a key result obtained by the Oak Ridge collaboration demonstrating that the effects of this improved treatment of nuclear electron capture are twofold. In regions close to the center of the star, the additional electron capture on heavy nuclei results in more electron capture in the new models. In regions where nuclei with  $A < 65$  dominate, the LMP rates result in less electron capture. The results of these competing effects can be seen in the first panel of Figure 4, which shows the distribution of  $Y_e$  throughout the core when the central density reaches  $10^{14} \text{ g cm}^{-3}$ , making the transition to nuclear matter. The combination of increased elec-

tron capture in the interior with reduced electron capture in the outer regions displaces the velocity minimum, which marks the eventual location of shock formation, by  $0.1 M_{\odot}$ . The full effects of these changes on the bounce and post-bounce evolution in supernova models will be discussed in [23, 24].

Our calculations clearly show that the many neutron-rich nuclei which dominate the nuclear composition throughout the collapse of a massive star also dominate the rate of electron capture. Astrophysics simulations have demonstrated that these rates have a strong impact on the core collapse trajectory and the properties of the core at bounce. The evaluation of the rates has to rely on theory as a direct experimental determination of the rates for the relevant stellar conditions (i.e. rather high temperatures) is currently impossible. Nevertheless it is important to experimentally explore the configuration mixing between *pf* and *sdg* shell in extremely neutron-rich nuclei as such understanding will guide and severely constrain nuclear models. Such guidance is expected from future radioactive ion-beam facilities.

The work has been partly supported by the Danish Research Council, by the Spanish MCYT under contract AYA2002-04094-C03-02, by NASA under contract NAG5-8405, by the National Science Foundation under contract AST-9877130, by the Department of Energy, through the PECASE and Scientific Discovery through Advanced Computing Programs and by funds from the Joint Institute for Heavy Ion Research. Oak Ridge National Laboratory is managed by UT-Battelle, LLC, for the U.S. Department of Energy under contract DE-AC05-00OR22725. JMS acknowledges the financial support of the “Fundação para a Ciência e Tecnologia”. HTJ and MR acknowledge support by the Sonderforschungsbereich 375 “Astro-Teilchenphysik” of the Deutsche Forschungsgemeinschaft. KL and HTJ thank the ECT\* in Trento, where part of this collaboration has been initiated, for its hospitality.

- 
- [1] G.M. Fuller, W.A. Fowler and M.J. Newman, *Astrophys. J. Suppl. Ser.* **42**, 447 (1980); *Astrophys. J. Suppl. Ser.* **48**, 279 (1982); *Astrophys. J.* **252**, 715 (1982)
  - [2] K. Langanke and G. Martínez-Pinedo, *Nucl. Phys. A* **673**, 481 (2000); *At. Data Nucl. Data Tables* **79**, 1 (2001).
  - [3] A. Heger *et al.*, *Phys. Rev. Lett.* **86**, 1678 (2001); *Astrophys. J.* **560**, 307 (2001)
  - [4] S. W. Bruenn, *Astrophys. J. Suppl.* **58**, 771 (1985); A. Mezzacappa and S. W. Bruenn, *Astrophys. J.* **405**, 637 (1993); **410**, 740 (1993)
  - [5] G. M. Fuller, *Astrophys. J.* **252**, 741 (1982)
  - [6] K. Langanke, E. Kolbe and D.J. Dean, *Phys. Rev. C* **63**, 032801 (2001)
  - [7] J. Cooperstein and J. Wambach, *Nucl. Phys. A* **420**, 591 (1984)

- [8] O. Sorlin *et al.*, Phys. Rev. Lett. **88**, 092501 (2002)
- [9] M.C. Vetterli *et al.*, Phys. Rev. C **45**, 997 (1992)
- [10] R.L. Helmer *et al.*, Phys. Rev. C **55**, 2802 (1997)
- [11] C. Johnson *et al.*, Phys. Rev. Lett. **69**, 3157 (1992); S.E. Koonin, D.J. Dean and K. Langanke, Phys. Rep. **278**, 2 (1997)
- [12] A. Mezzacappa *et al.*, Phys. Rev. Lett. **86**, 1935 (2001)
- [13] G.M. Fuller, W.A. Fowler and M.J. Newman, Astrophys. J. **293**, 1 (1985)
- [14] J. Lattimer and F.D. Swesty, Nucl. Phys. A **535**, 331 (1991).
- [15] W.R. Hix, Ph.D. thesis, Harvard University, 1995.
- [16] E. Bravo and D. García-Senz, Mon. Not. Roy. Ast. Soc. **307**, 984 (1999).
- [17] M.F. El Eid and W. Hillebrandt, Astron. & Astrophys. Suppl. Ser. **42**, 215 (1980).
- [18] F. Brachwitz *et al.*, Astrophys. J. **536**, 934 (2000).
- [19] K. Langanke, G. Martínez-Pinedo and J.M. Sampaio, Phys. Rev. C **64**, 055801 (2001).
- [20] M. Rampp and H.-Th. Janka, Astrophys. J. Lett. **539**, 33 (2000)
- [21] S. W. Bruenn and W. C. Haxton, Astrophys. J. **376**, 678 (1991).
- [22] J. M. Sampaio, K. Langanke, G. Martínez-Pinedo, and D. J. Dean, Phys. Lett. B **529**, 19 (2002)
- [23] W.R. Hix *et al.*, to be published
- [24] H.-Th. Janka *et al.*, to be published